Numerical Study of PCM Integration Impact on Overall Performances of a Highly Building-Integrated Solar Collector

F. Motte [a,*], G. Notton [a], Chr. Lamnatou [b], C. Cristofari [a], D. Chemisana [b]

[a] Research Centre Georges Peri, Laboratory Sciences for Environment, UMR CNRS 6134,
University of Corsica Pasquale Paoli, Route des Sanguinaires, F-20000 Ajaccio, France
[b] Applied Physics Section of the Environmental Science Department,
University of Lleida, c/Pere Cabrera s/n, 25001 Lleida, Spain

Abstract: Heat loss reduction and overall performances improvement of a solar thermal collector by using Phase Change Material (PCM) are examined. Thermal losses at high reduced temperatures were identified previously due to the specific BISTS shape. For limiting both temperature and thermal losses, a PCM addition is studied. As adding PCM might change the optimum operating conditions: the influence on monthly performances of existing PCM characteristics, flow rate, temperature regulation and PCM volume addition are investigated. Simulations for a complete DHWS was performed with measured environmental data. The model of PCM thermal process is presented. The performances with PCM addition are evaluated and the improvements are estimated. A Life Cycle Assessment is performed in order to examine the influence of PCM use on the environmental profile of the proposed solar system.

Introduction

The required energy to produce hot water represents only 6% of overall housing energy consumption, but with reduced heating needs mainly due to a better thermal insulation and new building regulation, the hot water production reaches sometimes 30% of energy consumption in a new housing. A solar collector can efficiently provide up to 80% of the hot water needs, without fuel cost or pollution and with a minimal O&M expense.

Solar thermal collectors are often seen as a foreign element of the building and many architects highlighted that building integration is a major issue in the development and spreading of solar technologies. Building integration is the combination of aesthetics and sustainability. Patented H2OSS concept was developed (Cristofari, 2006), studied (Motte, 2012) and presented (Motte *et al.*, 2013a; 2013b; Notton *et al.*, 2014). This BISTS is a solar water collector inserted within a drainpipe conserving its rainwater-evacuation role (Fig. 1) and it is invisible from the ground.

Fig. 1. Presentation of the studied BISTS.

The H2OSS BIST can be used whatever is the orientation of the wall because the collector is oriented south into the drainpipe. The canalizations connecting the house to the collector are hidden into the vertical drainpipe. An installation is made by several connected modules (1 m x 0.125 m). The BISTS was tested and modelled (Motte *et al.*, 2013a, 2013b), then numerically optimized (Notton *et al.*, 2014) after some design modification (number and position of water pipes, air layer thickness, thermal insulation thickness). The optimized version had improved thermal performances with an increase of the annual solar fraction from 41% to 76%. But, the

specific BISTS structure induces high thermal losses limiting its performances. The thermal insulation (rock wool) is now replaced partially by a Phase Change Material (PCM) for using it as thermal energy storage but mainly for limiting the water temperature and thus reducing the thermal losses.

An optimization study was presented (Notton *et al.*, 2014) and showed particularly that the water tubes (cold and hot) were incorrectly positioned. In this paper, the optimized configuration of the BISTS was chosen. In Fig. 2, a description of the solar collector is shown.
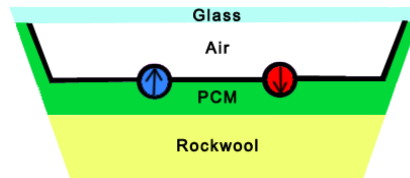
Fig. 2. Structure of the studied BISTS.

In the frame of this concept, the present paper includes:
- a numerical model of the solar domestic hot water system (SDHW) with PCM behavior;
- a presentation of the results and comparison with the actual configuration in terms of thermal performances – optimization of the solar collector configuration;
- a LCA for the two configurations, with and without PCM.

1. PCMs for solar thermal collectors and PCM selection

A solution, often described in literature for improving the efficiency of thermal systems is to use PCMs particularly in solar energy storage applications and in buildings applications in view to increase thermal inertia and by stabilizing the indoor climate with lower variation of temperature. Using PCMs reduces the lower mean temperature of the heating medium compared with a conventional fluid and this results in less heat losses.

A short literature review shows that if PCM increases the overall efficiency of a solar thermal collector, when placed directly into a classical solar collector, the results are strongly dependent on the configuration: collector, temperature, flow rate, user behaviour. The gain must be significant to justify to the higher complexity of the PCM system. Thus, the relative low thermal conductivity limits the performances. Here, a parametric study of adding some PCM into the collector is conducted in order to decrease the reduced temperature and the thermal losses.

A LCA provides useful information about the environmental profile of a BISTS (Lamnatou *et al.* 2014, 2015), this study examines the behaviour of this BISTS according to Energy Payback Time (EPBT), based on two scenarios (with/without PCM).

PCMs store the thermal energy by changing the enthalpy occurring during the phase transitions. This heat is absorbed or released during the transition phase from solid to liquid state or vice versa. At melting point temperature; specific for each material, the melting/freezing begins and absorbs/releases heat at constant temperature. Many parameters influence the choice of a PCM: cost, sensible and latent heat, melting point and heat conductivity in solid and liquid phases. The selection of the right PCM for any application requires the PCM to have a melting temperature within the practical range of application (between 50-55°C). Fig. 3 shows the PCM type vs. the melting point temperature (Zhou *et al.*, 2012). Among all the PCMs available in the literature, several PCMs were tested and 9 of them were chosen for being presented in this paper since they are the most efficient for our application. In Table 1, the main physical and thermal properties of these PCMs are shown.
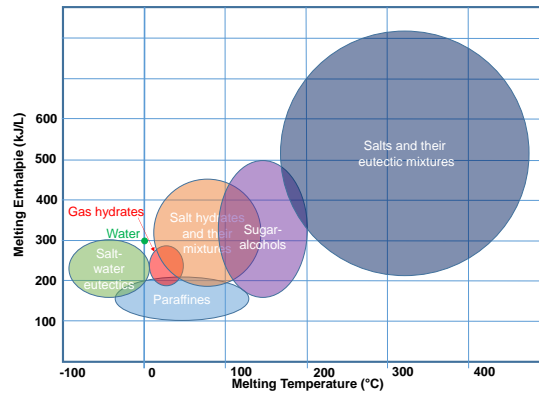
Fig. 3. Melting enthalpy and temperature for PCM groups (Zhou *et al*, 2012)

Table 1. Thermal characteristics of the 9 tested PCMs.

	Melting point temperature $T_{melting}$ (°C)	Enthalpy of fusion H (kJ.kg^{-1})	Thermal conductivity (W.m^{-1}.K^{-1})	Density (kg.m^{-3})	Specific heat C_p (kJ.kg^{-1}.°C^{-1})
61.5% Mg(NO$_3$)$_2$.6H$_2$O + 38.5% NH$_4$NO$_3$	52	125.5	0.5	1500	2.6
Paraffin C20-C3	50	189	0.21	850	2.5
Paraffin C22-C45	58	189	0.21	880	2.5
Myristic acid 54	54	189	0.17	844	3
Myristic acid 51	51	189	0.17	844	3
RT50	54	195	0.2	1300	0.93
RT52	52	138	0.2	900	0.2
STL 55	55	242	1	1290	2.5
STL + CENG	51	189	2.5	844	3

2. Numerical model of the collector and the SDHW

The thermal modeling consists in a thermal collector model calculating the output water and collector components temperatures-coupled to a water storage model (Haillot *et al.*, 2011).

The BISTS has its lateral faces much wider than a conventional collector relatively to its collecting surface (Fig. 1). Thus, its thermal behavior is different from one of usual solar collectors. A two-dimension model was developed for observing the temperatures evolution from meteorological data. It was tested and validated on a BISTS prototype with 9 temperature sensors (glass, blade, absorber, insulation, 2 faces, cold and hot water tubes).

The collectors are serial connected: the output fluid temperature of the first module becomes the input fluid temperature of the next one (Fig. 4). The RMSE calculated based on one-year data are around 5% for the water temperatures and between 4.6% and 10% for the internal ones.
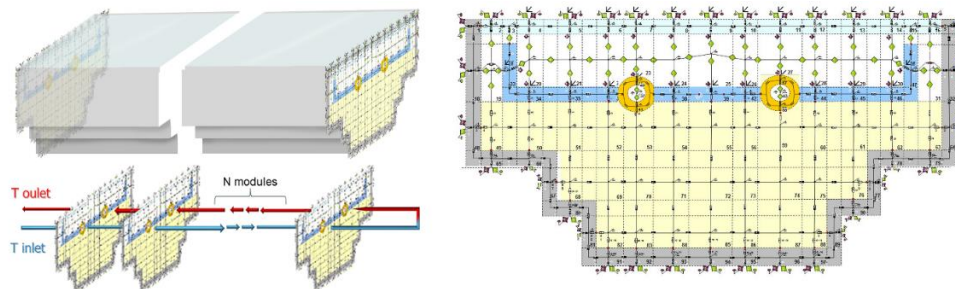
Fig. 4. The electrical analogy of the solar thermal collector and its serial connection.

The linear structure of the collector induces high hydraulic losses and the SDHW is operating with better performances in low flow rate conditions with other advantages such as:
-   thermal stratification of the water storage decreasing the auxiliary energy consumption and increasing the solar energy production;
-   utilization of smaller diameter pipes;

- reduced circulation pump consumption.

This thermal study concerns a SDHW used by a family of 4 persons in Corsica (France) and with 35 serial connected modules (4 m²) and a 200 L tank. The temperature into the thermal loop is simulated with a second numerical code based on a nodal approach (Fig. 5).
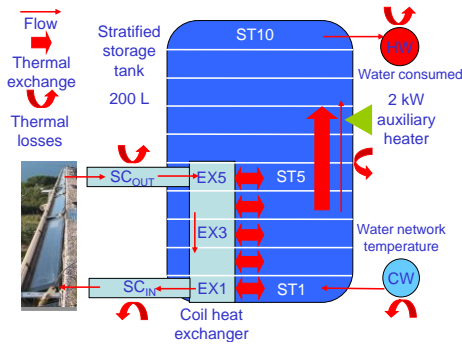
Fig. 5. SHDW model nodes   Fig. 6. Daily profile of drawing water
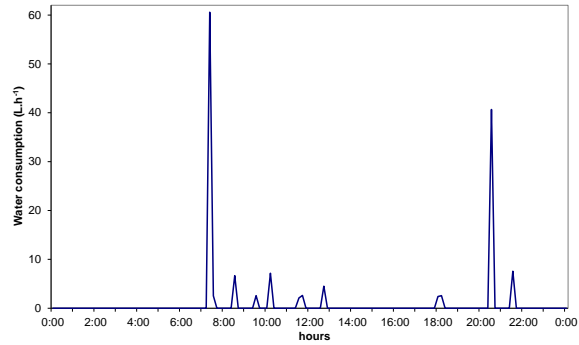
The coil heat exchanger is modelled by 5 nodes and the thermal exchanges between the heating fluid and the tank water are calculated using ε-NTU method (Shah and Mueller, 1985). In Fig. 6, the hot water consumption, given to the user at 50°C, is presented. A thermal flash at 70°C is produced one time per day to prevent the risk of legionella. The auxiliary heating and pumping operations are described in Motte *et al* (2013b).

A simplified model using a temperature-dependent function, describes the sensible and latent heats and defines a Gaussian distribution around the melting point (Akeiber *et al.*, 2016):

$$\text{if } T < T_{melting}, C_p = C_{S,solid}$$

$$\text{if } T_{melting} - \Delta T < T < T_{melting} + \Delta T , \ C_p = \left(H/\sigma\sqrt{2\pi}\right)exp\left[-\left(T - T_{melting}\right)^2 / 2.\sigma^2\right]$$

$$\text{if } T > T_{melting}, C_p = C_{S,liquid} \qquad \text{Eq. (1)}$$

with $C_{S,solid}$ and $C_{S,liquid}$ the sensible heats in solid and liquid states, H the melting latent heat, σ a constant used to set the width of the Gaussian. Here, σ is taken equal to 3 (Haillot, 2009).

4. Results and discussions

Three solar fractions SF, SF^+ and SF^{++} have been defined:
- SF: ratio of solar energy $E_{thermal,solar}$ and total thermal energy delivered to the tank $E_{thermal}$, sum of solar and auxiliary energies $E_{electical,AuxHeat}$ delivered to the tank.

$$SF = E_{Thermal,solar}/E_{Thermal} == E_{Thermal,solar}/\left(E_{Thermal,solar} + E_{Electical,AuxHeat}\right) \qquad \text{Eq. (2)}$$

- SF^+: high hydraulic losses occur due to modules serial connexion; a high power electrical pump is used. A new electrical energy $E_{electrical,pump}$ is added:

$$SF^+ = E_{Thermal,solar}/\left[E_{Thermal,solar} + E_{Electical,AuxHeat} + E_{Electrical,pump}\right] \qquad \text{Eq. (3)}$$

- SF^{++}: the "value" of electrical and thermal energy differs. The equivalence between these two energies is $\eta_{Ther-Elec}$=2.63 (Huang *et al*, 2001):

$$SF^{++} = E_{Thermal,solar}/\left[E_{Thermal,solar} + \left(E_{Electical,AuxHeat} + E_{Electrical,pump}\right)/\eta_{Ther-Elec}\right] \text{ Eq. (4)}$$

4.1. PCM influence on the reduced temperature

Fig. 7 shows the collector output water temperature for PCM and Rockwool versions for winter and summer for a 50 L.h^{-1}flow rate. The impact of PCM presence is to reduce the maximum reached temperature but no influence is seen on the performances. The output temperature is lower during the day in PCM version. During the night, it remains higher with increased thermal losses. The 'night' heat part is not used as it is colder than the storage tank one.
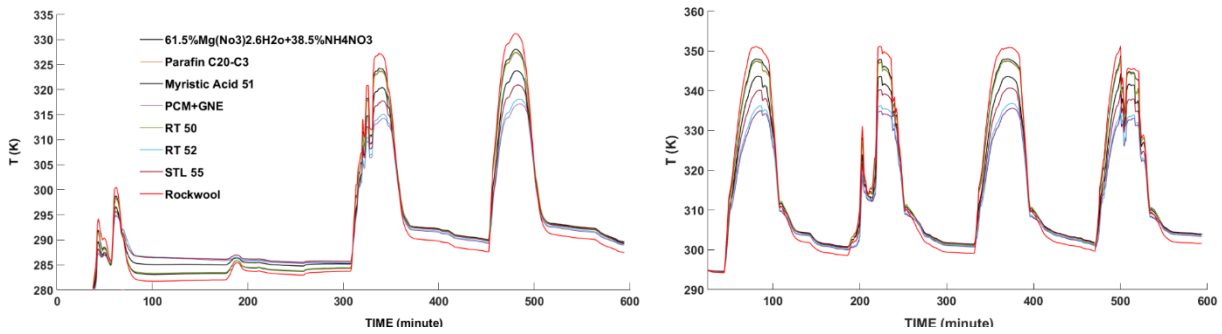
Fig. 7. Temperature variation for some typical days in January and July.

4.2. Monthly Solar fractions

In order to quantify the global performances of PCM configuration, simulations were performed over an entire year and month by month to examine the seasonal influence. Fig. 8 presents the monthly solar fractions SF++ for a complete year, for all the selected PCMs and without PCM.
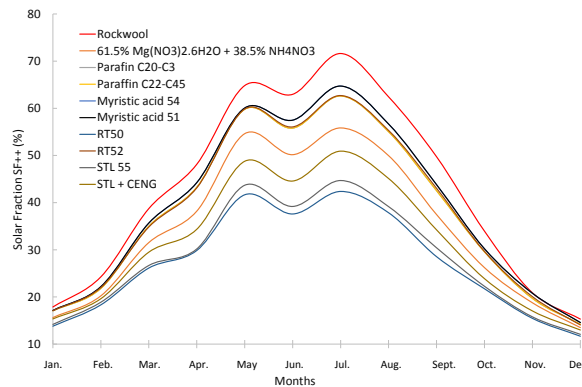
Fig. 8. Monthly evolution of SF^{++} for the tested PCMs.

For all selected PCMs, the original Rockwool configuration presents the best results for a flow-rate at 50 L.h^{-1} identified as optimal for the original version without PCM (Notton *et al.,* 2014). The best PCM version is obtained for the Myristic acid 51 identified previously by Hasan and Sayigh (1994) as a promising candidates for water heating. A similar behaviour is observed for SF and SF^{+} but with smaller gaps during winter and bigger gaps during summer.

Decreasing only water temperature and thermal losses does not lead to any improvement of the SDHW performances as a produced heat part stored in PCM is recovered efficiently. One efficient way to improve the overall performances is to adapt the dynamic behaviour of the installation to the PCM utilization. This dynamic behaviour is impacted mainly by flow rate.

4.3. Influence of the dynamic behaviour of the installation

4.3.1. Flow rate study

Flow-rate was optimised for the Rockwool version and it may be different for the PCM version. The best flow-rate for Myristic acid 51 version is researched. The solar fractions were calculated from 30 to 60 L.h^{-1} (Table 2). The optimum flow rate for the Rockwool version at 50 L.h^{-1} is confirmed (Notton *et al*, 2014). For the PCM version, the best results are obtained for a flow-rate of 45 L.h^{-1} and the performances are better than the Rockwool version. SF and SF^{++} increased by 1.16% (66.6% to 67.76%) and 2.56% (42.6% to 45.16%).

The PCM addition modifies the dynamic behaviour mainly by decreasing the temperature and increasing the collector inertia. This lower optimum flow rate allows to use a smaller pump explaining a higher gain for SF^{++} than SF (pump consumption taken into account).

Table 2. Solar fractions vs. flow-rates and performance improvements

Flow rates (L.h⁻¹)	Rockwool			Myristic Acid 51		
	SF %	SF+ %	SF++ %	SF (gain) %	SF+ (gain) %	SF++ (gain) %
30	55.45	51.32	35.6	56.31 (1.55)	52.45 (2.20)	36.8 (3.37)
40	61.6	58.0	39.0	61.98 (0.66)	58.75 (1.24)	40.15 (3.02)
42.5	63.7	60.1	40.4	63.53 (-0.33)	60.17 (0.17)	41.40 (2.59)
45	66.5	62.6	42.6	**67.76 (1.84)**	**64.32 (2.71)**	**45.16 (6.09)**
47.5	66.6	62.6	42.6	63.53 (-4.54)	59.81 (-4.51)	39.76 (-6.58)
50	66.6	62.6	42.6	63.41 (-4.74)	59.63 (-4.82)	38.96 (-8.46)
60	66.6	62.5	42.4	63.22 (-5.07)	59.27 (-5.16)	37.43 (-11.73)

Fig. 9 shows the monthly SF and the improvement compared with original version at 50 L.h⁻¹.
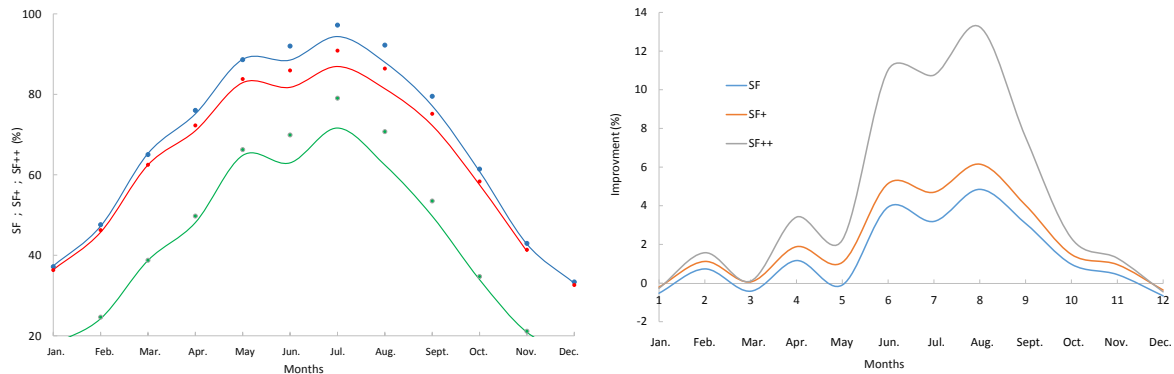
Fig. 9. Monthly solar fractions (Blue: SF; Red: SF+; Green SF++ for Rockwool configuration at 50 L.h⁻¹ (line) versus PCM configuration at 45 L.h⁻¹ (dots) and improvements.

June presents some untypical bad weather conditions, explaining the crush of performances. The annual gain is 1.16% (relative +1.74%) for SF, 1.72% (+2.75%) for SF^+ and 2.56% (+6%) for SF^{++}. The gain is significant in summer and slightly negative in winter as shown by Haillot *et al* (2009). The gain over the SF^{++} is more significant due to the double effect: increasing the performances while decreasing the pump consumption. PCM is clearly not solicited evenly throughout a whole year. During winter, PCM have some difficulties to reach the melting point or the temperature required to start the circulation of the pump.

4.3.2. Thickness of the PCM layer

The amount of PCM was changed from 0.5 to 3cm. Adding more or less PCM, increases or decreases its heat capacity, and influences its behaviour. As shown in Fig 4, the insulation is divided into 3 layers. A small performances improvement is noted with the replacement of Rockwool by PCM only situated into the first layer under the absorber (Table 3).

Table 3. The solar Fractions (in %) for different PCM thicknesses.

PCM thickness	½ layer	1 layer	2 layers	3 layers
SF	67.20	**67.76**	65.94	65.45
SF+	63.52	**64.32**	61.84	61.52
SF++	43.92	**45.16**	41.59	41.47

The best results are obtained for the first tested configuration: 1 cm of PCM under the absorber. Adding more and more PCM decreases a little bit the yearly performances by adding to much thermal inertia into the collector. Furthermore, the bottom part of PCM added is not solicited as much as the first layer. Adding less PCM, with a thickness decreased down to half a centimetre still increases the performances but the gain is smaller. So the selected configuration obtained is with a layer of 1 cm in contact under the absorber, with a flow rate of 45 L.h⁻¹.

5. Life Cycle Assessment (LCA)

The whole system including: 1) 35 solar modules with 2 scenarios A and B with and without PCM and additional components (storage tank, pump, external tubes with insulation, glycol).

The boundaries refer to the whole system in terms of phases of material manufacturing, system installation, use/maintenance, transportation and disposal. The assumptions for: glycol, impact of collector and materials manufacturing processes, impact of system installation, general maintenance, conversion of solar-system output into primary energy, are based on Lamnatou *et al.* (2014; 2015). The use phase includes replacement of some parts over its lifespan (25 years): one for the glass and the tank and five for glycol. For scenario B, PCM is replaced five times (Hasan and Sayigh, 1994). The inputs for pumping and auxiliary heating are taken into account during use/operational phase. A distance of 50 km is assumed for transportation (by lorry) and landfill is assumed as waste treatment. Cumulative Energy Demand (CED) (ecoinvent database, SimaPro 8) was used. The EPBT was calculated using equation presented by Lamnatou *et al.* (2014): 1) considering (case 1) or not (case 2) pump/auxiliary heating for $E_{O\&M.a}$, For pump/auxiliary heating, the electricity is provided by the mix of France. In Table 4, the life-cycle inventory is presented. For scenario B (with PCM), one additional component is added (Myristic acid: 28.73 kg) while the insulation (rock wool) is reduced from 8.09 kg (scenario A) to 5.70 kg (scenario B). The other components/materials/masses are the same for both scenarios.

Table 2. Life-cycle inventory: components/materials/masses for the 35 collectors (left) and additional components/materials/masses for the system (right).

For the 35 collectors	Mass (kg)	For the system	Mass (kg)
Black absorber (aluminium)	6.85	Storage tank (stainless steel)	31.20
Cover (glass)	49.59	Storage tank (rockwool)	10.20
Tube for cold water (copper)	8.86	Tubes (copper)	14.09
Tube for hot water (copper)	8.86	Tubes (polyurethane)	4.51
Insulation (rock wool)	8.09 (A)/5.70(B)	Propylene glycol	3.50
External casing (aluminium)	21.53	Pump (stainless steel)	3.00
PCM	28.73 (B)		
Two blades (polycarbonate)	1.68		
Polyester 1 (at the casing)	0.23		
Gutter (aluminium)	25.47		
Polyester 2 (at the gutter)	0.35		

In Fig. 4, the EPBTs are illustrated: 1) if pumping/auxiliary heating are not considered, the two scenarios «No PCM, 50 L/h» and «With PCM, 45 L/h» have almost the same EPBT, 2) if pumping/auxiliary heating are considered, the case A presents 0.6 years lower EPBT in comparison to the case B, 3) by considering pumping/auxiliary heating, the EPBT increases due to additional inputs during use/operational phase. Based on the EPBT energy metric, it is noted that even if PCM has an additional impact (in terms of material manufacturing, use phase, etc.), on a long-term basis, this additional impact (given the fact that PCM induces a 5 L/h reduction) is compensated. In all cases, the EPBTs show very lower values than system lifespan.
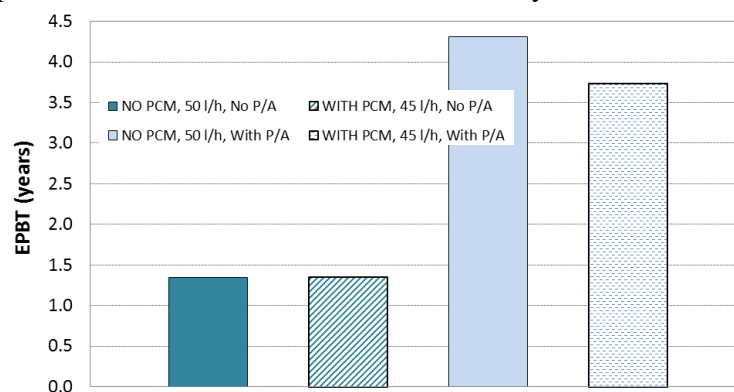
Fig. 4. EPBTs: «No PCM, 50 L/h» vs «With PCM, 45 L/h», «No P/A» (without taking into account P/A (pumping/auxiliary heating)) vs. «With P/A» (taking into account P/A).

Conclusions

Studies realized on the H2OSS collector showed that its specific shape induces high thermal and hydraulic losses, reducing its thermal performances. A PCM utilization was considered to decrease the working temperature and to reduce the heat losses. PCMs were reviewed and numerically tested: the most appropriate is Myristic acid 51. The performances are quantified in terms of solar fractions taking into account the electrical energy for pump operation. A decrease of the working temperature was clearly seen but no significant performances improvement was detected. The optimal flow rate was recalculated for the PCM version. With Myristic acid 51 and optimal conditions, the thermal performances have risen slightly in a yearly basis with a positive impact in summer and a small negative one in winter. Regarding LCA, for all cases the EPBTs are considerably lower than system lifespan (25 years).

References

Akeiber H., Nejat P., Abd. Majid M.Z., A. Wahid M., Jomehzadeh F., Famileh I.Z, et al. A review on phase change material (PCM) for sustainable passive cooling in building envelopes, Ren Sust Ener Rev 2016;60:1470–97.
Cristofari C. Device for Collecting Rainwater and Solar Energy Originating from Light Radiation, U.S. Patent WO 2006/100395 A12006.
Haillot D., Nepveu F., Goetz V., Py X., Benabdelkarim M. High performance storage composite for the enhancement of solar domestic hot water systems. Part 1 : Storage material investigation, Sol.Energy 2011;85-5:1021–7.
Haillot D., Nepveu F., Goetz V., Py X., Benabdelkarim M. Numerical model of a solar DHW including PCM media in the solar collector. Proc. Energy Studies – Effstock 2009.
Hasan A, Sayigh A.A. Some fatty acids as phase change thermal energy storage material. Ren. Energy 1994;4(1):69-76.
Huang B.J, Lin T.H., Hung W.C., Sun F.S. Performance evaluation of solar photovoltaic/thermal systems. Sol Energy 2001;70:443-8.
Lamnatou C., Notton G., Chemisana D., Cristofari C. Life cycle analysis of a building-integrated solar thermal collector, based on embodied energy and embodied carbon methodologies. Energ Build 2014;84:378-387.
Lamnatou C., Notton G., Chemisana D., Cristofari C. The environmental performance of a building-integrated solar thermal collector, based on multiple approaches and life-cycle impact assessment methodologies. Build Environ 2015;87:45-58.
Motte F. Study of a high building integrated solar collector. PhD thesis, University of Corsica Pasquale Paoli, 07/12/2012 (in French).
Motte F, Notton G., Cristofari C., Canaletti JL. A building integrated solar collector: performances characterization and first stage of numerical calculation. Ren Ener 2013a;49:1-5.
Motte F., Notton G., Cristofari C., Canaletti J.L. Design and modelling of a new patented thermal solar collector with high building integration. Appl Energy 2013b;102: 631-9.
Notton G., Motte F., Cristofari C., Canaletti J.L. Performances and Numerical Optimization of a Novel Thermal Solar Collector for Residential Building. Ren Sust Ener Rev 2014;33:60–73.
Shah K., Mueller A.C. Heat exchangers. In: Rohsenow WM, Hartnett JP, Ganic EN, editors. Handbook of heat transfer applications. New York: Mc Graw Hill; 1985.
Tiwari A., Sodha M.S. Performance evaluation of hybrid PV/thermal water/air heating system: an experimental validation. Solar Energy 2006b;80:751-9.
Zhou D., Zhao C.Y., Tian Y. Review on thermal energy storage with phase change materials (PCMs) in building applications. Applied Energy 2012;92:593-608.